Letter

Two-fermion negativity and confinement in the Schwinger model

Adrien Florio*

Department of Physics, Brookhaven National Laboratory, Upton, New York 11973

(Received 10 January 2024; accepted 14 February 2024; published 8 April 2024)

We consider the fermionic (logarithmic) negativity between two fermionic modes in the Schwinger model. Recent results pointed out that fermionic systems can exhibit stronger entanglement than bosonic systems, exhibiting a negativity that decays only algebraically. The Schwinger model is described by fermionic excitations at short distances, while its asymptotic spectrum is the one of a bosonic theory. We show that the two-mode negativity detects this confining, fermion-to-boson transition, shifting from an algebraic decay to an exponential decay at distances of the order of the de Broglie wavelength of the first excited state. We derive analytical expressions in the massless Schwinger model and confront them with tensor network simulations. We also perform tensor network simulations in the massive model, which is not solvable analytically, and close to the Ising quantum critical point of the Schwinger model, where we show that the negativity behaves as its bosonic counterpart.

DOI: 10.1103/PhysRevD.109.L071501

Introduction. Entanglement is a defining property of the quantum world. Understanding its structural impact on quantum many-body systems and quantum field theories is key. This was realized in the early days of modern quantum field theory [1]. It has led to a plethora of works, starting from the conjecture of the area law for the entanglement entropy [2], computation of the entanglement entropy in conformal field theory (CFT) [3], and in holography [4]. More than their intrinsic interests, these studies have led to reconsidering and gaining insights into old field theoretic questions and considering new problems. Examples range from understanding high-energy scattering in terms of entanglement [5–12], entanglement in pair production [13–16], the impact of entanglement structures on the renormalization group flow [17–21] and systematic construction of effective field theories [22–26], links to thermalization [27–33], and to partial and dynamical symmetry breaking and restoration [34–36], see also [37–39] for reviews on the interface of quantum information science and field theory.

To fully apprehend entanglement, the study of mixed states is crucial. From a many-body perspective, it allows, for instance, to probe entanglement between subsystems. In this case, entanglement measures are not unique. The (logarithmic) negativity is a useful one as it provides an upper bound on the amount of *distillable* entanglement, i.e. the amount of entanglement that can be recovered using local observables [40–44]. Its behavior has been extensively studied in CFTs [45–48] and was also explored in free scalar field theories [23–25]. Recently, Ref. [49] pointed out that fermionic degrees of freedom can carry more entanglement than bosonic degrees of freedom. In particular, they exhibited systems where the fermionic negativity decays only as a power law. This is in contrast to bosonic systems, as even close to critical points, the logarithmic negativity decays faster than any power [45,50]. Having fermionic excitations potentially more strongly entangled than bosonic excitations is interesting in relation to confining theories, where the spectrum of the theory is not made out of trivial excitations of the microscopic particles. It is suggestive that when a fermionic theory gives rise only to bosonic excitations, the spatial distribution of negativity should probe the scale at which the theory confines. As a result, an intriguing problem to investigate is the relationship between entanglement measures and confinement.

This work explores these ideas within the Schwinger model, quantum electrodynamics in $1+1$ dimensions:

$$H = \int \mathrm{d}x[\bar{\psi}(\gamma^1(-i\partial_1 + A_1) + m)\psi] + \frac{g^2}{2}E^2, \quad (1)$$

with A_1 the gauge potential, E is the canonically conjugate operator for the electric field and $\psi^T = (\psi_1\psi_2)$ is a two component spinor. Gauss's constraint supplements it, $\partial_1 E = \bar{\psi}\gamma^0\psi \equiv \psi^\dagger\psi$ with $\bar{\psi} \equiv \psi^\dagger\gamma^0$. It manifests the remaining "gauge invariance" of the Hamiltonian formalism. We express the γ matrices in terms of Pauli matrices as $\gamma^0 = \sigma_z$, $\gamma^1 = -i\sigma_y$, $\gamma^5 = \gamma^0\gamma^1 = -\sigma_x$.

*aflorio@bnl.gov

It is an ideal playground to test these ideas as it is known to be dual to a bosonic scalar theory and that asymptotic excitations of the model, "mesons," are bosons (they are solitons made out of the scalar field) [51,52]. In other words, it behaves as a fermionic theory only over the shortest scales and transitions to a bosonic behavior at larger scales. Moreover, when the mass parameter m vanishes, the bosonic theory is simply a *massive* free scalar field with mass $m_b = g/\sqrt{\pi}$ [53]. In this case, the theory is analytically solvable.

We will study a standard fermionic chain that approaches the Schwinger model in the continuum. It can be constructed by introducing "staggered fermions" [54,55]

$$\chi_{2j} = \sqrt{2a}\psi_1(x_j), \qquad \chi_{2j+1} = \sqrt{2a}\psi_2(x_j). \tag{2}$$

As depicted in Fig. 1, lattice sites are labeled by an integer $n = 1, \ldots, 2N$. A physical site is made out of two lattice sites. The upper component of the continuum spinors lives on odd sites, while the down component lives on even sites. Physical distances are measured in units of $1/2a$ with a the lattice spacing. We impose open-boundary conditions on the fermions $\chi_0 = \chi_{2N+1} = 0$. In this setting, the remaining gauge freedom allows to set the gauge potential to zero and express the electric field only in terms of fermionic operators by solving Gauss law, see for instance [56] for explicit expressions. The resulting Hamiltonian reads

$$H_S^L = -\frac{i}{2a}\sum_{n=1}^{N-1}[\chi_n^\dagger\chi_{n+1} - \chi_{n+1}^\dagger\chi_n] + m\sum_{n=1}^{N}(-1)^n\chi_n^\dagger\chi_n + \frac{ag^2}{2}\sum_{n=1}^{N-1}\left(\sum_{i=1}^{n}Q_i\right)^2, \tag{3}$$

with $Q_i = n_i(1-(-1)^i)$ the lattice charge density operator and $n_i = \chi_i^\dagger\chi_i$ the fermion number operator.

We will investigate the two-fermion (logarithmic) negativity. After defining it and studying its behavior in the continuum, we show that it indeed transitions from an algebraic decay at small distances to an exponential decay at large distances. Moreover, the transition happens precisely at the de Broglie wavelength of the first bosonic excited state. We conclude by investigating the behavior of the logarithmic fermionic negativity at the quantum Ising critical point of the Schwinger model. We show that even when using a fermionic description, the bosonic expectation of the theory is met, and the negativity decays exponentially fast.

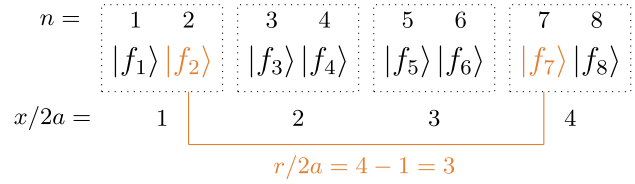

FIG. 1. Staggered set-up in the Schwinger model. Physical sites are made out of two lattice sites. The difference from a spinful "electron" is that gauge fields, before being integrated out, also link fermions within a physical site. We consider here the negativity between even/odd modes; the same analysis can be repeated for the odd/odd or even/even correlations.

Two-fermion negativity and the continuum limit. We start from the simple realization that a tractable expression for the density matrix for two staggered modes can be written down explicitly in terms of the staggered fields' two- and four-point functions [49,57,58]. We consider the reduced density matrix between modes whose physical sites are separated by a physical distance r and are equally distant from the center of the lattice, as depicted in Fig. 1. Because of the staggering, the sites are not related by a reflection symmetry, and we need a generalization of [49]. Consider the state $|\psi\rangle = \sum_{i_1,\ldots,i_{2N}=0,1} c_{i_1,\ldots,i_{2N}}|i_1,\ldots,i_{2N}\rangle$. The reduced density matrix obtained after tracing all sites except j and k reads

$$\rho_{j\leftrightarrow k} = \sum_{i'_j,i'_k,i_j,i_k=0,1}\Lambda_{i'_ji'_k,i_ji_k}|i'_ji'_k\rangle\langle i_ji_k|,$$
$$\Lambda_{i'_ji'_k,i_ji_k} = \sum_{\substack{\{i_l\}=0,1\\ l\neq j,k}} c^*_{i_1,\ldots i_j,\ldots i_k,\ldots,i_{2N}}c_{i_1,\ldots ij\prime,\ldots i'_k,\ldots,i_{2N}}. \tag{4}$$

The matrix elements $\Lambda_{i'_ji'_k,i_ji_k}$ can be expressed in terms of the fermion fields' two- and four-point functions. We restrict ourselves to states with zero total charge $Q = 0$. As a result, the density matrix takes the following form

$$\rho_{j\leftrightarrow k} = \begin{pmatrix} \Lambda_{00,00} & 0 & 0 & 0 \\ 0 & \Lambda_{01,01} & \Lambda_{01,10} & 0 \\ 0 & \Lambda^*_{01,10} & \Lambda_{10,10} & 0 \\ 0 & 0 & 0 & \Lambda_{11,11} \end{pmatrix}. \tag{5}$$

Direct computations give

$$\langle n_j\rangle_\psi = \Lambda_{10,10} + \Lambda_{11,11}, \qquad \langle n_k\rangle_\psi = \Lambda_{01,01} + \Lambda_{11,11},$$
$$\langle n_jn_k\rangle_\psi = \Lambda_{11,11}, \qquad \langle\chi_j^\dagger\chi_k\rangle_\psi = \Lambda_{01,10}, \tag{6}$$

using the shorthand notation $\langle\ldots\rangle_\psi \equiv \langle\psi|\ldots|\psi\rangle$. Thus, using (6) and $\mathrm{Tr}(\rho_{j\leftrightarrow k}) = 1$ in the occupation number basis $\{|00\rangle, |01\rangle, |10\rangle, |11\rangle\}$, we have,

$$\Lambda_{00,00} = 1 - \langle n_j\rangle_\psi - \langle n_k\rangle_\psi + \langle n_jn_k\rangle_\psi,$$
$$\Lambda_{10,10} = \langle n_j\rangle_\psi - \langle n_jn_k\rangle_\psi, \qquad \Lambda_{11,11} = \langle n_jn_k\rangle_\psi,$$
$$\Lambda_{01,01} = \langle n_k\rangle_\psi - \langle n_jn_k\rangle_\psi, \qquad \Lambda_{01,10} = \langle\chi_j^\dagger\chi_k\rangle_\psi.$$

We need the fermionic partial transpose of (5) to compute the negativity. Following [59], it acts on our two-fermion reduced Hilbert space as

$$(|i'_ji'_k\rangle\langle i_ji_k|)^{T_j^f} = (-1)^\alpha|i_ji'_k\rangle\langle i'_ji_k|,$$
$$\alpha = \frac{i'_j(i'_j+2)}{2} + \frac{i_j(i_j+2)}{2} + i_ki'_k + i'_ji'_k + i_ji_k + (i_j+i_k)(i'_j+i'_k). \tag{7}$$

It leads to

$$\rho^{T_j}_{j\leftrightarrow k} = \begin{pmatrix} \Lambda_{00,00} & 0 & 0 & i\Lambda^*_{01,10} \\ 0 & \Lambda_{01,01} & 0 & 0 \\ 0 & 0 & \Lambda_{10,10} & 0 \\ i\Lambda_{01,10} & 0 & 0 & \Lambda_{11,11} \end{pmatrix}, \quad (8)$$

with eigenvalues $\lambda_1, \lambda_2, \lambda_+, \lambda_-$:

$$\lambda_1 = \Lambda_{01,01}, \qquad \lambda_2 = \Lambda_{10,10},$$
$$\lambda_\pm = \frac{1}{2}\Big(1 - \Lambda_{01,01} - \Lambda_{10,10} \pm \sqrt{-4|\Lambda_{01,10}|^2 + (-\Lambda_{00,00} + \Lambda_{11,11})^2}\Big). \quad (9)$$

The eigenvalues $\lambda_{1,2}$ are real and positive. We can take $\lambda_\pm = \lambda_R \pm i\lambda_I$ with $\lambda_I \neq 0$ as when they are real, they are also positive, as shown in the Supplemental Material [60]. Then,

$$\mathcal{N}^{2f} \equiv \sum_{i\in\{1,2,+,-\}} \frac{|\lambda_i| - \lambda_i}{2} = |\lambda_\pm| - \lambda_R, \quad (10)$$

$$\epsilon_{\mathcal{N}^{2f}} \equiv \log(1 + 2\mathcal{N}^{2f}) = \log(1 + 2(|\lambda_\pm| - \lambda_R)), \quad (11)$$

with $\mathcal{N}^{2f}$ the two-fermion negativity and $\epsilon_{\mathcal{N}^{2f}}$ the corresponding two-fermion logarithmic negativity. These simple expressions allow us to investigate what happens in the continuum limit. We focus on the ground state of the Schwinger model. First, we recover translational invariance. Then, $\langle n_x\rangle = 1/2$ as the vacuum state of the field theory corresponds to half-filling in terms of the staggered fermions. For the same reason, the correlator that has a continuum limit is the connected two-point function of $\langle \delta n_j \delta n_k\rangle$ (equivalent to "normal ordering" in the continuum theory). Taking x_j and x_k the physical points associated with j and k, see Fig. 1, we write its continuum limit $n_2(r)$, with $r = x_j - x_k$ (it can be expressed in terms of the vector charge and the chiral condensate, but it won't be used here). Lastly, $\langle \chi^\dagger_j \chi_k\rangle$ converges to appropriate components of the continuum, full equal time correlator of the theory $D_{\alpha\beta}(r)$. In more detail, we have, depending on their parity,

$$\begin{pmatrix} \langle \chi^\dagger_{2x_j}\chi_{2x_k}\rangle & \langle \chi^\dagger_{2x_j}\chi_{2x_k+1}\rangle \\ \langle \chi^\dagger_{2x_j+1}\chi_{2x_k}\rangle & \langle \chi^\dagger_{2x_j+1}\chi_{2x_k+1}\rangle \end{pmatrix} \to \begin{pmatrix} D_{11}(r) & D_{12}(r) \\ D_{21}(r) & D_{22}(r) \end{pmatrix}. \quad (12)$$

This is how the fact that the Dirac propagator in the continuum is a two-by-two matrix manifests itself in the staggered formulation.

Reinstating the correct factors of a according to (2), we have

$$\lambda_{1,2} \to \frac{1}{4} - 2a^2 n_2$$
$$\lambda_\pm \to \frac{1}{4} - 2a^2 n_2 \pm 2ia^2 D_{\alpha\beta}. \quad (13)$$

Note that, notwithstanding the continuum analysis, it matches the results of [49] around half-filling.

Now, we are in a position to study the continuum behavior of the two-fermion negativity. Plugging this in (10), we find

$$\mathcal{N}^{2f}_{\alpha\beta}/a^2 \to 8|D_{\alpha\beta}|^2 + O(a^2). \quad (14)$$

The fact that the two-fermion negativity vanishes as a^2 can easily be explained. The quantity with a continuum limit without any rescaling by factors of a is the one between two subsystems of a given physical length. As $a \to 0$, the number of modes contained in each subsystem grows as $1/a$. By insisting on computing the negativity between single modes, we need to pay a factor of $1/a^2$ in (14). The indices α, β reflect the fact you can consider the negativity between the same component modes or opposite component modes. Note that this relation to the propagator is reminiscent of the results of [61], where the quantum Fisher information, another measure of multipartite entanglement, was successfully probed using single particle propagators only.

What is insightful is that the continuum limit of $\mathcal{N}^{2f}_{\alpha\beta}/a^2$ is simply proportional to the square propagator between the two modes. It gives a new interpretation to the space-like part of the propagator in this kind of field theory: it measures the two-mode entanglement in the system. It also strengthens the speculation made in the introduction. The two-fermion negativity detects confinement, at least in one dimension. More generally, it is suggestive that entanglement measures can be used to probe confinement, exhibiting different behavior when probing asymptotically free degrees of freedom with respect to scattering states.

Massless schwinger model. We exemplify these ideas by studying first the massless Schwinger model. The continuum theory is dual to the theory of a massive free boson ϕ of mass $m_b = g/\sqrt{\pi}$ [53]. The fermionic propagator is known explicitly [62,63]

$$D_{11}(r) = D_{22}(r) \equiv d_1(r) = \frac{m_b}{4\pi} e^{G(r)+\gamma_E}, \quad (15)$$

$$D_{12}(r) = D_{21}(r) \equiv d_2(r) = \frac{m_b}{4\pi} e^{G(r)+K_0(m_b r)+\gamma_E}, \quad (16)$$

$$G(r) = -m_b^2 \int_0^\infty \frac{\mathrm{d}k}{\sqrt{k^2 + m_b^2}} \frac{\sin^2(\frac{kr}{2})}{k^2} \quad (17)$$

with $r = x - y$, K_0 the 0^{th} Bessel function of the second kind. They both admit simple asymptotes

$$d_1(r) \sim \begin{cases} \frac{m_b}{4\pi} e^{\gamma_E}, r \to 0 \\ \frac{m_b}{4\pi} e^{\frac{1}{2}+\gamma_E - \frac{m_b \pi r}{4}}, r \to \infty \end{cases}, \quad (18)$$

$$d_2(r) \sim \begin{cases} \frac{1}{2\pi r}, r \to 0 \\ \frac{m_b}{4\pi} e^{\frac{1}{2}+\gamma_E - \frac{m_b \pi r}{4}}, r \to \infty \end{cases}, \quad (19)$$

with γ_E the Euler-Mascheroni constant. As was pointed out early on [62], the fermionic propagator captures the transition from a free constituent fermionic theory at small distances to a massive bosonic free bosonic theory at large distances, where the propagator is screened.

We now show that the two-fermion negativity defined from the lattice model indeed approaches the square propagator. To compute the negativity from the lattice model, we performed tensor network simulations using the ITensor library [64,65]. We compute the ground state using DMRG and evaluate the negativity with (10). To minimize finite-size effects, and for all simulations presented in this work, we use the improved lattice mass parameter of [66]. We show the even/odd negativity $\mathcal{N}_{12}^{2f}$ normalized by a^2 for a fixed coupling in Fig. 2. We also fix the physical volume such that finite-volume effects are negligible. The colored curves correspond to different lattice spacings and represent taking the continuum limit (with $N = 100$, 200, and 400 staggered sites). The gray curve is the analytical prediction (14). As claimed in the previous section, the negativity systematically approaches the norm square of the propagator. The transition from the algebraic fermionic behavior to the exponentially decreasing bosonic one is sharp and happens at the boson radius $1/m_b$. Note the deviations from the analytical prediction at a large radius are due to approaching the boundaries of our lattice (we use open-boundary conditions). It is a concrete example where the two sites' fermionic negativity transitions from an algebraic decay to an exponential one. This transition probes confinement. We will see that it still happens in massive case which is not analytically solvable.

The same analysis can, in principle, be repeated for the even/even or odd/odd case. In practice, some staggered discretization artifacts that cancel in the even/odd case make the even/even and odd/odd negativity zero for the range of lattice spacings studied here, and non-zero only closer to the continuum, see Supplemental Material [60] for more detail. Consequently, we will restrict ourselves to studying the even/odd negativity for the rest of this work.

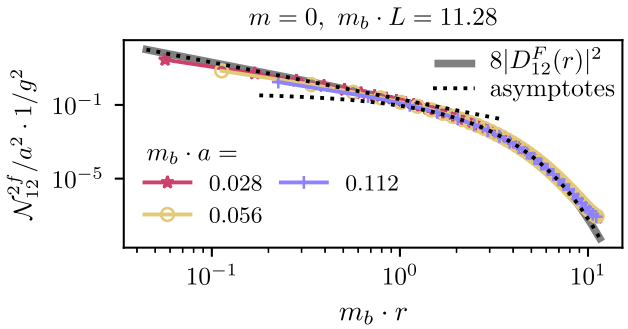

FIG. 2. The deviations at small r are lattice artifacts, as demonstrated by the apparent convergence to the analytical result as $a \to 0$. The deviations from the analytical prediction at large r are due to boundary effects. The different lattice spacings correspond to lattices of $N = 100$, 200, 400 staggered sites.

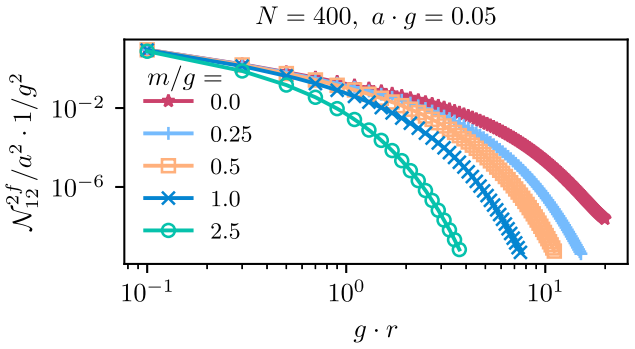

FIG. 3. Two-fermion negativity as a function of distance, for different m/g ratios. All curves transition from an algebraic to an exponential decay.

Massive schwinger model. We now move on to the massive Schwinger model, which is not known to be analytically solvable. It is dual to an interacting bosonic theory [52]. We repeat our DMRG simulation for the same g value as in the massless case for different mass parameters. We show the resulting negativities in Fig. 3. The transition from an algebraic behavior to an exponential decay is still clear. It happens at shorter distances for larger masses. We show the same data in Fig. 4, rescaling the x and y axis in terms of the mass gap. For the three smaller ratios of m/g, we used the values of [67], which we checked against our own determination of the mass gap obtained by targeting the first excited state. For the larger mass, the leading prediction $m_{1st}^2 = m_b^2 + m^2$ is accurate at the percent level [67] and was used to estimate the gap. We observe a relatively good collapse, showing that the leading dependence of the negativity is the mass of the first excited state. In particular, the transition from an algebraic behavior to an exponential decay happens in all cases at $r \sim 1/m_{1st}$, and thus is sensitive to the typical confinement length at which the theory transitions from being fermionic to bosonic.

Massive schwinger model at criticality. The Schwinger model is critical for negative masses at the critical mass to

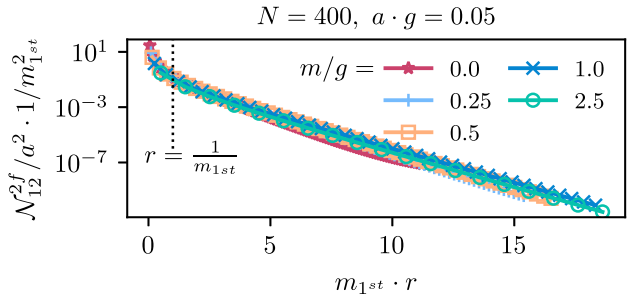

FIG. 4. Two-fermion negativity as a function of distance, for different m/g ratios, with the axis scaled by appropriate powers of the mass gap. The curves' approximate collapse indicates that the negativity's main dependence is on the mass gap. The transition from the algebraic fermionic decay to the bosonic exponential one happens at $r \sim 1/m_{1st}$, indicated by a dotted black line.

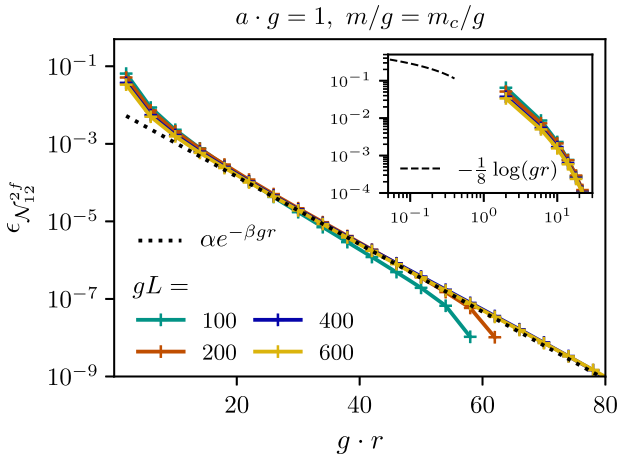

FIG. 5. Two-fermion logarithmic negativity at the critical mass. At large distances, the fermionic negativity still decays exponentially, as expected for the $2D$ Ising CFT. The dashed line is the result of a fit to an exponential $\alpha e^{-\beta gr}$ with $\alpha = 0.00786 \pm 0.00023$ and $\beta = 0.20051 \pm 0.00075$. Inset: while out-of-reach of the data presented here, the behavior of $\epsilon_{\mathcal{N}}$ also seems consistent with the small r prediction $\epsilon_{\mathcal{N}} \sim -c/4\log(gr)$ with $c = 1/2$ the central charge of the $2D$ Ising CFT.

coupling ratio $m_c/g \approx 0.3335$ [68,69] and is in the $2D$ Ising universality class. Reference [49] showed that fermionic CFTs can exhibit logarithmic negativity that decays algebraically, in contrast to bosonic CFTs where the logarithmic negativity is known to decay faster than any polynomials [45,50]. An interesting feature of the massive Schwinger model is that it is a fermionic representation of a bosonic CFT, and it is thus of value to investigate the behavior of the fermionic logarithmic negativity in this model. Results are shown in Fig. 5. The system is tuned at its second-order critical point. The two-fermion logarithmic negativity is plotted as a function of distance. The different curves correspond to different volumes. The dashed line is a fit to an exponential decay. In this case, the fermionic negativity is also exponentially suppressed at large distances; it behaves in the same way as the bosonic one. This matches expectations from universality, as the underlying CFT has no knowledge of fermionic operators.

We found the small distance behavior to be out of reach of the specific numerical methods used in this work; we show the small r behavior of our data in the inset of Fig. 5. We also plot the universal Ising expectation for very small r. While far from the regime of applicability of this prediction, it appears that our data do not contradict this small distance behavior. This regime can be better studied using dedicated tensor network simulations more appropriate to critical systems [70,71].

Discussion. We studied in this work the two-fermion (logarithmic) negativity of fermionic spin chains and its behavior in the continuum limit. In particular, we focused on the Schwinger model. While expressible purely as a fermionic chain, it has the interesting property of being fermionic only at short distances, while a bosonic scalar theory describes its asymptotic spectrum. We showed that the negativity is sensitive to this "confinement radius," at which it transitions from an algebraic decay to an exponential one. We also showed that the fermionic negativity behaves as its bosonic counterpart at the Ising critical point of the massive Schwinger model, as universality would suggest.

These results are interesting from two different perspectives. First, it is an explicit example where the fermionic negativity exhibits a transition from a more entangling, in the sense of [49], fermionic behavior to a bosonic behavior at large distances, as would be expected by bosonization. It shows that the fermionic negativity captures the system's fundamental statistics and does not measure an artifact related to the representation of the system's degrees of freedom. Second, it further motivates us to think about how confinement relates to entanglement and how entanglement measures can be used to probe it. Moreover, the explicit relation between the two-fermion negativity and the full propagator of the theory is intriguing and invites reflection on how entanglement measures between physical subregions can be systematically related to field theoretical n-point functions.

This work opens other natural outlooks. A simple extension would be to consider how the two-mode negativity is affected when computed between two full Dirac fermions (four modes negativity in a staggered formulation or two-site negativity for Wilson fermions). Considering its behavior in the presence of localized states is also an interesting avenue. More challenging, investigating the two-mode density matrix in the presence of dynamical gauge fields will be an essential step in generalizing these results to higher dimensions and more realistic theories.

Acknowledgment. The author thanks João Barata for interesting discussions, Erik Gustafson for speeding up his code, and Robert Szafron for insightful discussions on negativity. The author is also grateful to Dmitri Kharzeev, Robert Pisarski, Robert Szafron, and Raju Venugopalan for comments on a draft of this manuscript. The author is supported by the U.S. Department of Energy under contract No. DE-SC0012704 and by the U.S. Department of Energy, Office of Science, National Quantum Information Science Research Centers, Co-design Center for Quantum Advantage (C^2QA), under contract No. DE-SC0012704.

[1] H. Reeh and S. Schlieder, Bemerkungen zur unitäräquivalenz von lorentzinvarianten feldern, Nuovo Cimento **22**, 1051 (1961).

[2] Mark Srednicki, Entropy and area, Phys. Rev. Lett. **71**, 666 (1993).

[3] Pasquale Calabrese and John L. Cardy, Entanglement entropy and quantum field theory, J. Stat. Mech. 06 (2004) P06002.

[4] Shinsei Ryu and Tadashi Takayanagi, Holographic derivation of entanglement entropy from AdS/CFT, Phys. Rev. Lett. **96**, 181602 (2006).

[5] Dmitri E. Kharzeev and Eugene M. Levin, Deep inelastic scattering as a probe of entanglement, Phys. Rev. D **95**, 114008 (2017).

[6] Dmitri E. Kharzeev and Eugene Levin, Deep inelastic scattering as a probe of entanglement: Confronting experimental data, Phys. Rev. D **104**, L031503 (2021).

[7] Wenjie Gong, Ganesh Parida, Zhoudunming Tu, and Raju Venugopalan, Measurement of Bell-type inequalities and quantum entanglement from Λ-hyperon spin correlations at high energy colliders, Phys. Rev. D **106**, L031501 (2022).

[8] Wibe A. de Jong, Kyle Lee, James Mulligan, Mateusz Płoskoń, Felix Ringer, and Xiaojun Yao, Quantum simulation of nonequilibrium dynamics and thermalization in the Schwinger model, Phys. Rev. D **106**, 054508 (2022).

[9] Adrien Florio, David Frenklakh, Kazuki Ikeda, Dmitri Kharzeev, Vladimir Korepin, Shuzhe Shi, and Kwangmin Yu, Real-time nonperturbative dynamics of jet production in Schwinger model: Quantum entanglement and vacuum modification, Phys. Rev. Lett. **131**, 021902 (2023).

[10] Ron Belyansky, Seth Whitsitt, Niklas Mueller, Ali Fahimniya, Elizabeth R. Bennewitz, Zohreh Davoudi, and Alexey V. Gorshkov, High-energy collision of quarks and mesons in the Schwinger model: From tensor networks to circuit QED, Phys. Rev. Lett. **132**, 091903 (2024).

[11] João Barata, Wenjie Gong, and Raju Venugopalan, Real-time dynamics of hyperon spin correlations from string fragmentation in a deformed four-flavor Schwinger model, arXiv:2308.13596.

[12] Kyle Lee, James Mulligan, Felix Ringer, and Xiaojun Yao, Liouvillian dynamics of the open Schwinger model: String breaking and kinetic dissipation in a thermal medium, Phys. Rev. D **108**, 094518 (2023).

[13] Adrien Florio and Dmitri E. Kharzeev, Gibbs entropy from entanglement in electric quenches, Phys. Rev. D **104**, 056021 (2021).

[14] Gerald V. Dunne, Adrien Florio, and Dmitri E. Kharzeev, Entropy suppression through quantum interference in electric pulses, Phys. Rev. D **108**, L031901 (2023).

[15] Sebastian Grieninger, Dmitri E. Kharzeev, and Ismail Zahed, Entanglement in a holographic Schwinger pair with confinement, Phys. Rev. D **108**, 086030 (2023).

[16] Sebastian Grieninger, Dmitri E. Kharzeev, and Ismail Zahed, Entanglement entropy in a time-dependent holographic Schwinger pair creation, Phys. Rev. D **108**, 126014 (2023).

[17] Robert C. Myers and Aninda Sinha, Seeing a c-theorem with holography, Phys. Rev. D **82**, 046006 (2010).

[18] Horacio Casini, Marina Huerta, and Robert C. Myers, Towards a derivation of holographic entanglement entropy, J. High Energy Phys. 05 (2011) 036.

[19] H. Casini and Marina Huerta, On the RG running of the entanglement entropy of a circle, Phys. Rev. D **85**, 125016 (2012).

[20] Horacio Casini, Eduardo Testé, and Gonzalo Torroba, Markov property of the conformal field theory vacuum and the a theorem, Phys. Rev. Lett. **118**, 261602 (2017).

[21] Gabriel Cuomo, Zohar Komargodski, and Avia Raviv-Moshe, Renormalization group flows on line defects, Phys. Rev. Lett. **128**, 021603 (2022).

[22] Silas R. Beane, David B. Kaplan, Natalie Klco, and Martin J. Savage, Entanglement suppression and emergent symmetries of strong interactions, Phys. Rev. Lett. **122**, 102001 (2019).

[23] Natalie Klco and Martin J. Savage, Geometric quantum information structure in quantum fields and their lattice simulation, Phys. Rev. D **103**, 065007 (2021).

[24] Natalie Klco and Martin J. Savage, Entanglement spheres and a UV-IR connection in effective field theories, Phys. Rev. Lett. **127**, 211602 (2021).

[25] Natalie Klco, D. H. Beck, and Martin J. Savage, Entanglement structures in quantum field theories: Negativity cores and bound entanglement in the vacuum, Phys. Rev. A **107**, 012415 (2023).

[26] Pablo Bueno, Horacio Casini, Oscar Lasso Andino, and Javier Moreno, Conformal bounds in three dimensions from entanglement entropy, Phys. Rev. Lett. **131**, 171601 (2023).

[27] Dmitri Kharzeev and Kirill Tuchin, From color glass condensate to quark gluon plasma through the event horizon, Nucl. Phys. **A753**, 316 (2005).

[28] Jürgen Berges, Stefan Floerchinger, and Raju Venugopalan, Dynamics of entanglement in expanding quantum fields, J. High Energy Phys. 04 (**2018**) 145.

[29] Zhao-Yu Zhou, Guo-Xian Su, Jad C. Halimeh, Robert Ott, Hui Sun, Philipp Hauke, Bing Yang, Zhen-Sheng Yuan, Jürgen Berges, and Jian-Wei Pan, Thermalization dynamics of a gauge theory on a quantum simulator, Science **377**, abl6277 (2022).

[30] Niklas Mueller, Torsten V. Zache, and Robert Ott, Thermalization of gauge theories from their entanglement spectrum, Phys. Rev. Lett. **129**, 011601 (2022).

[31] Lukas Ebner, Berndt Müller, Andreas Schäfer, Clemens Seidl, and Xiaojun Yao, Eigenstate Thermalization in $2+1$ dimensional SU(2) Lattice Gauge Theory, Phys. Rev. D **109**, 014504 (2024).

[32] Xiaojun Yao, SU(2) gauge theory in $2+1$ dimensions on a plaquette chain obeys the eigenstate thermalization hypothesis, Phys. Rev. D **108**, L031504 (2023).

[33] Sebastian Grieninger, Kazuki Ikeda, Dmitri E. Kharzeev, and Ismail Zahed, Entanglement in massive Schwinger model at finite temperature and density, Phys. Rev. D **109**, 016023 (2024).

[34] Filiberto Ares, Sara Murciano, and Pasquale Calabrese, Entanglement asymmetry as a probe of symmetry breaking, Nat. Commun. **14**, 2036 (2023).

[35] Filiberto Ares, Sara Murciano, Eric Vernier, and Pasquale Calabrese, Lack of symmetry restoration after a quantum quench: An entanglement asymmetry study, SciPost Phys. **15**, 089 (2023).
[36] Filiberto Ares, Sara Murciano, Lorenzo Piroli, and Pasquale Calabrese, An entanglement asymmetry study of black hole radiation, arXiv:2311.12683.
[37] Tatsuma Nishioka, Entanglement entropy: Holography and renormalization group, Rev. Mod. Phys. **90**, 035007 (2018).
[38] Natalie Klco, Alessandro Roggero, and Martin J. Savage, Standard model physics and the digital quantum revolution: thoughts about the interface, Rep. Prog. Phys. **85**, 064301 (2022).
[39] Christian W. Bauer, Zohreh Davoudi, Natalie Klco, and Martin J. Savage, Quantum simulation of fundamental particles and forces, Nat. Rev. Phys. **5**, 420–432 (2023).
[40] Asher Peres, Separability criterion for density matrices, Phys. Rev. Lett. **77**, 1413 (1996).
[41] Pawel Horodecki, Separability criterion and inseparable mixed states with positive partial transposition, Phys. Lett. A **232**, 333 (1997).
[42] R. Simon, Peres-Horodecki separability criterion for continuous variable systems, Phys. Rev. Lett. **84**, 2726 (2000).
[43] G. Vidal and R. F. Werner, Computable measure of entanglement, Phys. Rev. A **65**, 032314 (2002).
[44] M. B. Plenio, Logarithmic negativity: A full entanglement monotone that is not convex, Phys. Rev. Lett. **95**, 090503 (2005).
[45] Pasquale Calabrese, John Cardy, and Erik Tonni, Entanglement negativity in quantum field theory, Phys. Rev. Lett. **109**, 130502 (2012).
[46] Pasquale Calabrese, John Cardy, and Erik Tonni, Entanglement negativity in extended systems: A field theoretical approach, J. Stat. Mech. 02 (2013) P02008.
[47] Sara Murciano, Riccarda Bonsignori, and Pasquale Calabrese, Symmetry decomposition of negativity of massless free fermions, SciPost Phys. **10**, 111 (2021).
[48] Sara Murciano, Vittorio Vitale, Marcello Dalmonte, and Pasquale Calabrese, Negativity Hamiltonian: An operator characterization of mixed-state entanglement, Phys. Rev. Lett. **128**, 140502 (2022).
[49] Gilles Parez and William Witczak-Krempa, Are fermionic conformal field theories more entangled?, arXiv:2310.15273.
[50] S. Marcovitch, A. Retzker, M. B. Plenio, and B. Reznik, Critical and noncritical long-range entanglement in Klein-Gordon fields, Phys. Rev. A **80**, 012325 (2009).
[51] Sidney R. Coleman, R. Jackiw, and Leonard Susskind, Charge shielding and quark confinement in the massive Schwinger model, Ann. Phys. (N.Y.) **93**, 267 (1975).
[52] Sidney R. Coleman, More about the massive Schwinger model, Ann. Phys. (N.Y.) **101**, 239 (1976).
[53] Julian S. Schwinger, Gauge invariance and mass. 2, Phys. Rev. **128**, 2425 (1962).
[54] John B. Kogut and Leonard Susskind, Hamiltonian formulation of Wilson's lattice gauge theories, Phys. Rev. D **11**, 395 (1975).
[55] Leonard Susskind, Lattice fermions, Phys. Rev. D **16**, 3031 (1977).
[56] Kazuki Ikeda, Dmitri E. Kharzeev, and Yuta Kikuchi, Real-time dynamics of Chern-Simons fluctuations near a critical point, Phys. Rev. D **103**, L071502 (2021).
[57] Younes Javanmard, Daniele Trapin, Soumya Bera, Jens H. Bardarson, and Markus Heyl, Sharp entanglement thresholds in the logarithmic negativity of disjoint blocks in the transverse-field Ising chain, New J. Phys. **20**, 083032 (2018).
[58] Clément Berthiere and William Witczak-Krempa, Entanglement of skeletal regions, Phys. Rev. Lett. **128**, 240502 (2022).
[59] Hassan Shapourian, Ken Shiozaki, and Shinsei Ryu, Partial time-reversal transformation and entanglement negativity in fermionic systems, Phys. Rev. B **95**, 165101 (2017).
[60] See Supplemental Material at http://link.aps.org/supplemental/10.1103/PhysRevD.109.L071501 for more details on the positiveness of the real eigenvalues and the continuum limit.
[61] Rajesh K. Malla, Andreas Weichselbaum, Tzu-Chieh Wei, and Robert M. Konik, Detecting multipartite entanglement patterns using single particle Green's functions, arXiv:2310.05870.
[62] A. Casher, John B. Kogut, and Leonard Susskind, Vacuum polarization and the quark parton puzzle, Phys. Rev. Lett. **31**, 792 (1973).
[63] James V. Steele, J. J. M. Verbaarschot, and I. Zahed, The invariant fermion correlator in the Schwinger model on the torus, Phys. Rev. D **51**, 5915 (1995).
[64] Matthew Fishman, Steven R. White, and E. Miles Stoudenmire, The ITensor software library for tensor network calculations, SciPost Phys. Codebases (**2022**) 4.
[65] Matthew Fishman, Steven R. White, and E. Miles Stoudenmire, Codebase release 0.3 for ITensor, SciPost Phys. Codebases (**2022**) 4.
[66] Ross Dempsey, Igor R. Klebanov, Silviu S. Pufu, and Bernardo Zan, Discrete chiral symmetry and mass shift in the lattice Hamiltonian approach to the Schwinger model, Phys. Rev. Res. **4**, 043133 (2022).
[67] C. Adam, Improved vector and scalar masses in the massive Schwinger model, Phys. Lett. B **555**, 132 (2003).
[68] T. Byrnes, P. Sriganesh, R. J. Bursill, and C. J. Hamer, Density matrix renormalization group approach to the massive Schwinger model, Nucl. Phys. B, Proc. Suppl. **109**, 202 (2002).
[69] T. Byrnes, P. Sriganesh, R. J. Bursill, and C. J. Hamer, Density matrix renormalization group approach to the massive Schwinger model, Phys. Rev. D **66**, 013002 (2002).
[70] Guifre Vidal, Entanglement renormalization: An introduction, arXiv:0912.1651.
[71] Jacob C. Bridgeman and Christopher T. Chubb, Hand-waving and interpretive dance: An introductory course on tensor networks, J. Phys. A **50**, 223001 (2017).